J. Marine Sci. Appl. (2016) 15: 484-492
DOI: 10.1007/s11804-016-1385-3

Effect of pH on Mechanical, Physical and Tribological Properties of Electroless Ni-P-Al_2O_3 Composite Deposits for Marine Applications

Sahil Julka, Mohd Imran Ansari and Dineshsingh G. Thakur*

Department of Mechanical Engineering, Defence Institute of Advanced Technology (DU), Pune-411025, India

Abstract: Successful co-deposition of fine particulate matter within an Electroless Nickel-Phosphorous (ENi-P) matrix is dependent on various factors like bath composition, particle compatibility with metallic matrix, bath reactivity (pH), particle size and their distribution. ENi-P deposits incorporating Al_2O_3/ Alumina in a disperse phase have varied effects on properties and attributes like surface roughness (*Ra*), microhardness, wear resistance, corrosion resistance and surface morphology of the deposits obtained. This paper experimentally investigates the effect of alumina (1.55 g/L) on *Ra*, microhardness, surface morphology, deposition rate, wettability, wear resistance and corrosion resistance of ENi-P-Al_2O_3 composite deposits on mild steel substrates at bath pH 5, 7 and 9. Study reveals that optimum deposit parameters and deposition rates are achieved with bath pH. However, not much study has been undertaken concerning composite deposits obtained from higher bath pH or basic bath. This is attributable to the fact that at higher bath pH or alkaline baths, the bath gets unstable and eventually degrades or decomposes, thereby resulting in sub optimal or poor deposition. Hence, experimental investigations carried out by preparing suitable baths, operating under optimum conditions, and enabling successful composite deposition in acidic and alkaline baths have revealed that there is a significant improvement in the above mentioned properties of the as-deposited composite deposits, as the pH is increased from pH 5 to pH 9. This aspect can therefore be advantageously utilized for preparing various marine components like fasteners, nuts, bolts, washers, pipes, cables, components having relative motion etc.

Keywords: ENi-P-Al_2O_3, composite deposits, pH, microhardness, surface roughness, deposition rate, wettability, wear resistance, corrosion resistance

Article ID: 1671-9433(2016)04-0484-09

1 Introduction

Mild steel, which is also referred to as plain carbon or low carbon steel makes up the largest part of steel production, and is used in a vast range of applications. The American Iron and Steel Institute defines a carbon steel as having no more than 2% carbon and no other appreciable alloying element. Typically, carbon steels are stiff and strong, and they also exhibit ferromagnetism. This means they are extensively used in motors and electrical appliances, in addition to manufacturing of washers, washers, screws, fasteners, pipes, nuts, bolts, hinges, cables etc. The corrosion resistance of carbon steels is poor and so they should not be used in a corrosive environment unless some form of protective deposition is used.

Electroless Nickel-Phosphorous (ENi-P) deposition technique, which is based on the principle of autocatalytic deposition process, is one such technique that is likely to sharply influence and enhance the properties of MS, including improvement in corrosion and wear resistance, microhardness, average surface roughness, thereby broadening its applications even in corrosive environment. These properties are further enhanced by incorporation of other metals, non-metals, abrasive particles or their combinations to the Ni-P matrix, thereby resulting in better prevention and improved resistance to failure under varying loads by forming composite deposits. Electroless Ni-P composite deposition forms a protective barrier coating, protecting the base substrate from corrosive environments. In this respect, ENi-P deposits with high phosphorous content offer maximum corrosion resistance as against medium or low phosphorous deposits (Gawrilov, 1979; Mallory and Hajdu, 1990; Baudrand, 1994). Several particles have been incorporated into Ni-P matrix to date, and amongst them, the ones which have gained maximum recognition and wide range of applications are electroless nickel with SiC (Islam *et al.*, 2015b), SiO_2 (Islam *et al.*, 2015a), Al_2O_3 (Islam *et al.*, 2013) and PTFE (Grosjean *et al.*, 2000).

Extensive literature survey on incorporation of nanoparticles into electroless nickel based coatings reveals that addition of silicon carbide (SiC) nanoparticles improves both corrosion resistance and mechanical properties of the resulting Ni-P/SiC nanocomposite coatings, thereby making them potential candidate as protective coatings in aggressive environments. The incorporation also resulted in smaller nodule size with fine-grain structure, low surface roughness, excellent corrosion resistance and sharp rise in average hardness values of the coated surface (Islam *et al.*, 2015b). Although pure medium and high phosphorous coatings offer a good combination of mechanical and corrosion properties,

Received date: 2016-01-30
Accepted date: 2016-06-28
***Corresponding author Email:** dineshsingh_thakur@yahoo.com

their performance attributes can be further enhanced through incorporation of silica (SiO_2) nanoparticles. Incorporation of silica (SiO_2) into ENi-P deposits result in superior corrosion resistance and average hardness, in addition to grain refinement, reduction in the surface roughness and minimization of surface porosity in the nanocomposite coatings (Islam *et al.*, 2015a). Studies also reveal that addition of nanostructures such as nanoparticles of alumina (Al_2O_3) or silicon carbide (SiC) or multi-walled carbon nanotubes (CNT) into Ni–P matrix, lead to a sharp rise in the corrosion resistance and microhardness values of the nano composite coating (Islam *et al.*, 2013).

Study has also been undertaken regarding the effect of bath pH on the coating or deposits properties on various base substrates. Electrochemical Impedance Spectroscopy (EIS) was used in combination with other techniques to investigate the role played by the pH of the chromate bath on the properties of the chromate film formed on Alclad 2024 aluminium alloy. Scanning Electron Microscopy (SEM), Atomic Force Microscopy (AFM) and Spectroscopic Ellipsometry (SE) have shown the formation of a thicker and less dense chromate layer when the pH of the chromate bath is changed from 2.4 to 1.2, thereby resulting in improved corrosion resistance view formation of more protective and more resistant Chromate Corrosion Products (CCP) inside the defects of the chromate film. However, on decreasing the pH to a too low value decreases the corrosion resistance effectiveness view negative effect of the increase in coating porosity (Campestrini *et al.*, 2002). The effect of bath pH values on the rate of electroless copper deposited from the tartarate bath and EDTA bath has also been studied, wherein the bath pH values were changed by the addition of NaOH concentrated solution to the electroless baths. The results indicate that the deposition rate increases markedly with the increase of pH value up to 12.5 for tartarate bath and 13.0 for EDTA bath. On going beyond these pH values, the rates of electroless plating decrease. Electroless copper baths are characterized by a plating rate that firstly increases and passes through a peak then begins to decrease as a function of pH (Hanna *et al.*, 2003).

By virtue of various favorable properties like high wear resistance, strength retention at high temperatures and high modulus of elasticity (Balaraju *et al.*, 2003), Al_2O_3/Alumina has been selected as second phase particles for incorporation into Ni-P matrix in the current analysis, thereby eventually leading to improved deposit characteristics resulting in better service life and higher levels of resistance to failure. The highlighting aspects leading to realization or incorporation of Al_2O_3 particles as second phase particles onto the substrate surface (MS in the present analysis) subjected to electroless deposition are bath reactivity/pH, particle impingement on the deposit/substrate surface and the holding time of particle on deposit surface (Apachitei *et al.*, 1998; Ger and Hwang, 2002). Rate and percentage of particle deposition, surface roughness (*Ra*), wettability and microhardness of ENi-P-Al_2O_3 composite deposits on the other hand depends on the alumina concentration in the bath. Increase in bath alumina concentration leads to an increase in the average roughness and hardness (Aal *et al.*, 2007). The effect of varying bath pH on ENi-P-Al_2O_3 composite deposits has not been greatly studied to date. Aim of the present investigation is to experimentally investigate the effect of different bath pH on microhardness, surface roughness (*Ra*), deposition rate, wettability, surface morphology, wear resistance, corrosion resistance and elemental analysis of ENi-P-Al_2O_3 composite deposits. Literature survey reveals that too low or lower bath pH is likely to result in poor deposition rate, deposit dullness and dark deposits on the as-deposited surface. Higher or too high bath pH on the other hand results in high surface roughness and instability of the bath solution. Barring a few exceptions, the ideal operating pH range for an acid Ni-P plating bath would be about 5.0 to 7.0 (Sahoo and Das, 2011). Further, several studies indicate that optimum ENi-P deposition rates are obtained for a bath pH value ranging between 4–5. However, it may be noted that the above values of bath pH have been highlighted considering deposition undertaken in acidic baths. This is attributable to the fact that higher bath pH has resulted in bath degradation or bath decomposition, thereby resulting in sub optimal deposition onto the base the substrate. Hence, in order to experimentally investigate the effect of acidic and alkaline baths on ENi-P composite deposits, efforts have been made to prepare a suitable bath, operating under optimum conditions that would enable successful composite deposition, both in acidic and alkaline range. Hence, in order to achieve optimum results, and experimentally investigate the outcome of varying bath pH on the characteristics of the as-deposited substrates, the bath pH has been maintained at 5, 7 and 9, while keeping the other parameters constant, for obtaining ENi-P-Al_2O_3 composite deposits.

2 Method and experimental details

2.1 Experimental setup and substrate preparation

The experiment comprised of ENi-P-Al_2O_3 chemical bath along with a Spinot hotplate to provide adequate amount of heat energy to the bath constituents to obtain the required composite deposit. The substrate used was mild steel specimen with circular cross section of 20 mm diameter and 5 mm thickness with a pin hole drilled close to the circumference (for ease of suspension in the chemical bath). As surface preparation of the base substrate is pivotal in determining the health of the resultant deposition, the substrate was subjected to a number of activities as a part of surface preparation, to enable successful deposition. The substrate was mechanically cleaned to ensure removal of physical particles/dust, followed by degreasing in acetone. The substrate was thereafter cleaned in 10% NaOH solution at 60 °C, post which the substrate was dipped in 10 mL of 40% by volume HCl for 02 resulting in etching. This ensured thorough removal of any rust particles from the

substrate surface. Finally the substrate was subjected to activation with 50 g/L of NaH_2PO_2 for 10 min, post which the substrate was subjected to deposition in the chemical bath for a duration of 80 min. Rinsing of the substrate with distilled water, after each surface preparation activity, and after deposition, was undertaken without fail.

2.2 Bath composition and operating conditions

Bath composition and operating conditions were selected after several experiments. The chemical bath used for ENi-P-Al_2O_3 composite deposit comprised of nickel sulphate as the metal ion (Ni^{+2}) source and sodium hypophosphite monohydrate acting as the reducing agent. Oxidation of reducing agent is responsible for producing electrons for reduction of Ni^{+2} ions onto the substrate surface. The bath also contained citric acid monohydrate, sodium susscinate and lead acetate, which are potential complexing agent, accelerator and stabilizer/inhibitor respectively. Role of the complexing agent is to prevent decomposition of the chemical bath, and addition of accelerator in small quantities leads to an increase in the deposition rate. Stabilizers play an important role in increasing the brightness of the composite deposits (Balaraju and Seshadri, 1999; Alirezaei *et al.*, 2004). The bath was operated for duration of 80 min with three different bath pH levels. The bath pH was maintained at pH 5, pH 7 and pH 9 for the three baths A, B and C respectively, prior to commencement of composite deposition onto the substrate. Though the bath comprised of the same constituents and in equal amounts, the pH was regulated by gradual addition of Sodium Hydroxide (NaOH) solution, prepared by mixing distilled water with NaOH pellets in a beaker. The addition of NaOH solution resulted in an increase in the bath pH which was measured using pH testing strips or paper. The bath pH was set to desired value by addition NaOH solution in the bath and testing the same using pH testing strips before carrying out ENi-P composite deposition on the base substrate. However, generation of hydrogen during the deposition process lowers the bath pH (Sudagar *et al.*, 2013). Hence, to maintain the bath pH as desired, pH testing strips were continuously dipped into the bath, at intervals on 05 minutes to detect any decrease in bath pH. The decrease in bath pH, if any, was increased up to desired levels by adding alkaline salt of Na or NaOH solution in present investigation, and cross checking using pH strips. The bath constituents, along with quantities, bath pH and operating conditions for obtaining ENi-P-Al_2O_3 composite deposits were maintained as given in Table 1.

2.3 Deposition rate and analysis of ENi-P-Al_2O_3 composite deposits

The as-deposited substrate was dried and weighed repeatedly until no further change in the reading was observed to ensure complete drying of the ENi-P-Al_2O_3 composite deposit. Based on the literature survey, the deposition rate, D, of the ENi-P-Al_2O_3 composite deposit, which is expressed in terms of weight gain, has been calculated using the following well established and tested formula:

$$D=\frac{W_2-W_1\times10^4}{\rho\times A\times T} \tag{1}$$

where D is the deposition rate (μ/h), W_1 is the weight of substrate before deposit (g), W_2 is the weight of substrate after deposit (g), ρ is the density of the deposit (g/cm^3), A is the surface area exposed to deposit (cm^2), and T is the deposition time in hours.

Table 1 Bath constituents and operating conditions of baths A, B and C

Bath constituents and operating conditions	Bath A	Bath B	Bath C
Nickel sulphate hexahydrate/(g·L^{-1})	25	25	25
Sodium hypophosphite monohydrate/(g·L^{-1})	20	20	20
Citric acid monohydrate/(g·L^{-1})	15	15	15
Sodium susscinate/(g·L^{-1})	16	16	16
Al_2O_3/(g·L^{-1})	1.55	1.55	1.55
pH	5	7	9
Temperature/°C	85±2	85±2	85±2
Deposit time/min	80	80	80

To study the surface morphology of composite deposits, Field Emission Scanning Electron Microscope (FESEM) (Model: Σigma, Carl Ziess) was used, and the composition of the deposits, i.e., weight percentage of nickel and phosphorus content in composite deposits was analyzed by Energy Dispersive X-Ray (EDX) analysis. Microhardness of composite deposits was estimated using Wilson Hardness Tester (Model Name- Tukon 1202) with Vickers diamond indenter, using 200 gm load for 10 seconds dwell time. Five trials were carried out per substrate to determine the microhardness values. The average surface roughness (*Ra*) of the deposited samples was measured using surface roughness gauge comprising of a stylus type profilometer on a micro scale and by using Atomic Force Microscope (AFM) comprising of a silicon cantilever for the tapping mode to measure the average surface roughness on a nano scale. Contact angle plays a vital role wherever the intensity of phase contact between liquid and solid substances needs to be assessed such as in applications like deposit, painting, cleaning, printing etc. The contact angle (Model: KRUSS GmBh, Germany) was measured using the image of a sessile drop at the points of intersection (three-phase contact points) between the drop contour and the projection of the surface (baseline). The measurements were carried out at ambient temperature with DI water as probe liquid. Each contact angle was recorded as an average of five measurements on the same sample/specimen. Tribometer wear tester machine (Magnum Engineers) was used to analyze the wear characteristics of composite deposited samples wherein a pin-on-disc type wear tester was used to carry out wear

testing. Each deposited sample was tested for 300 s with a counter disc of EN31 material with a Rockwell hardness of 55–60 HRC. The disc rpm was maintained at 100 r/min with a track radius of 20 mm and loading of 20 N without lubrication. The tester provides graphical results and displays the wear parameters directly after the defined test duration. At the end of each test, the wear track substrates were examined in FESEM. The corrosion rate, thereby, reflecting the corrosion resistance of the as-deposited samples was analysed against chloride attack in a salt water spray chamber (Make - Advance Equipments). In order to assess the corrosion resistance against chloride attack, the as-deposited specimens were subjected to accelerated corrosion test in an aggressive salty environment in accordance with ASTM and ISO standards. The Salt Water Spray Chamber is ideal for testing the rust resistance grade and corrosion resistance of specimens post surface treatments like electroless deposition, paint coating and anodizing. The as-deposited specimens obtained from baths A, B and C were exposed to salt spray in the Salt Water Spray Chamber. The specimens were thoroughly degreased with acetone and rinsed in deionized water before corrosion testing. The time taken for appearance of rust on the as-deposited surface was carefully recorded so as to assess the corrosion rate of each specimen. The corrosion rate was calculated using the weight loss method and is expressed as millimeter per year (mm/a). The mathematical equation for calculating the corrosion rate is given as (Syed, 2006):

$$\text{Corrosion rate (mm/a)} = \frac{87.6 \times W}{\rho \times A \times T} \quad (2)$$

where W is the weight loss (mg), ρ the density of specimen (g/cm^3), A the area of specimen (cm^2), and T the exposure time in hours.

3 Results and discussion

The ENi–P deposit structure and properties, in general, primarily depends upon the phosphorous content present in the deposit. Hence, in order to analyze the effect of varying bath pH and co-deposition of alumina particles on the chemical composition of composite deposits, EDX analysis has been carried out. Fig. 1 shows the EDX analysis images of ENi-P-Al_2O_3 composite deposits obtained from baths A, B and C. A sharp variation in phosphorus and nickel content was noticed in the composite deposits obtained from baths A, B and C. The wt % of phosphorous in composite deposits from baths A, B and C are 7.11, 14.79 and 9.51 respectively, and that of nickel is 92.79, 80.51 and 65.18 respectively. The alumina incorporation onto the substrate also increased from 0.1% to 25.32% as the pH varied from 5 to 9 respectively. Thus, this is clearly indicative of the fact that the chemical composition of the ENi-P-Al_2O_3 composite deposit is sharply influenced with the changing bath pH and bath pH plays a major role in controlling the incorporation of alumina (Al_2O_3) in the deposit.

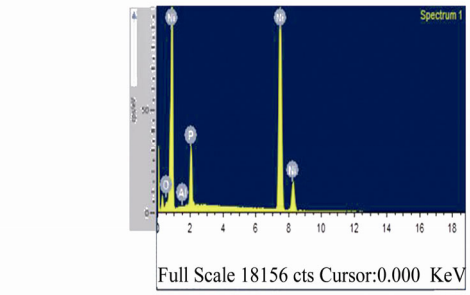

(a) Baths A

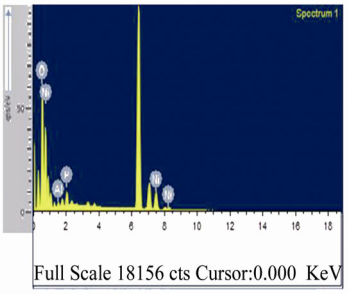

(b) Bath B

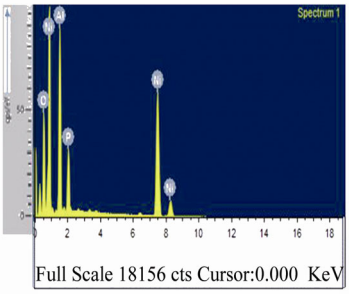

(c) Bath C

Fig. 1 EDX analysis of ENi-P-Al_2O_3 composite deposit

The surface morphology of Ni-P-Al_2O_3 composite deposits was studied using FESEM. The comparison of the morphology of the as-deposited substrates obtained from baths A, B and C are as shown in Fig. 2. It is evident from the figure that deposit obtained from the bath with pH 5/bath A show a irregular grain pattern with a rather small grain size and with negligible alumina/Al_2O_3 content. The deposit however shows minimum phosphorous concentration of 7.11% and maximum nickel concentration of 92.79%, thereby having enhanced wear resistance (Apachitei *et al.*, 1998). The increased phosphorous content however results in increased corrosion resistance of the deposit. From the deposit obtained from bath B, it is evident that the nodular structure of Ni is visible along with distinct grain boundaries and larger grain size. The deposition of phosphorus is observed to be distinctively higher than that observed in the deposits obtained from bath A and C, as against nickel, which is observed to be lower than that obtained from bath A. The aluminium content in the deposit has however increased as the bath pH has been varied from 5 to 7. With bath pH at 9 (bath C), the phosphorus content is observed to be uniformly distributed, however lower in concentration, thereby providing good wear resistance. The deposit thus obtained has distinctive nodular structure of Ni with

maximum grain size as compared to deposits obtained in baths A and B. The deposit obtained from bath C has the maximum aluminium content. This aspect can be taken into account while designing marine components wherein wear and corrosion play an extremely vital role.

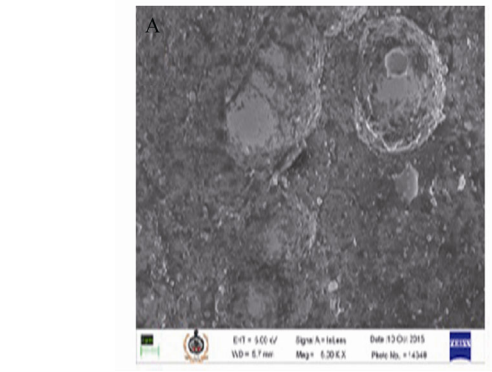

(a) Baths A

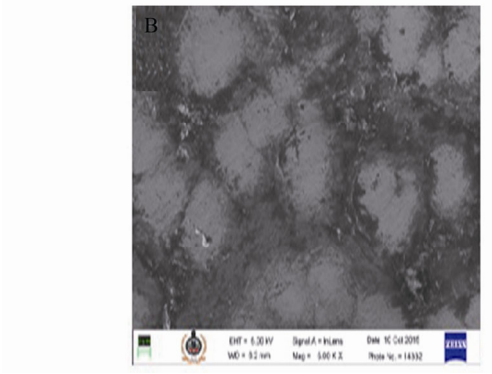

(b) Bath B

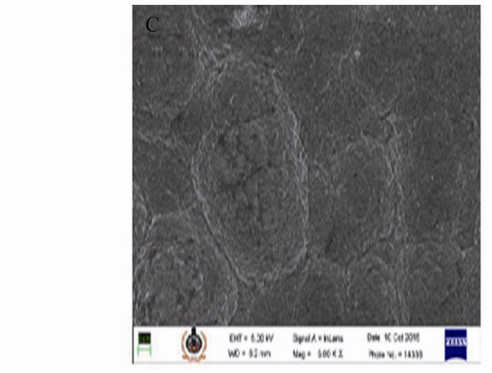

(c) Bath C

Fig. 2 FESEM morphology of ENi-P-Al_2O_3 composite deposit

Table 2 Properties and attributes of as-deposited substrates obtained form baths A, B &C

Property	Bath A	Bath B	Bath C
Average *Ra*/nm	36	47	66
Deposition rate/ ($\mu m \cdot h^{-1}$)	12.28	20.46	24.57
Microhardness/Hv	261	490	625
Contact angle/(°)	77.2	79.7	99.2
Film or deposition thickness/μm	16.38	27.30	32.76

The variation of average surface roughness (*Ra*) value at different bath pH was calculated with the help AFM by using the silicon cantilever for the tapping mode and the values obtained have been shown in Table 2, in addition to graphical representation in Fig. 3.

Fig. 4 shows the three-dimensional AFM images for the as deposited ENi-P-Al_2O_3 composite deposits, deposited for duration of 80 min on mild steel substrate.

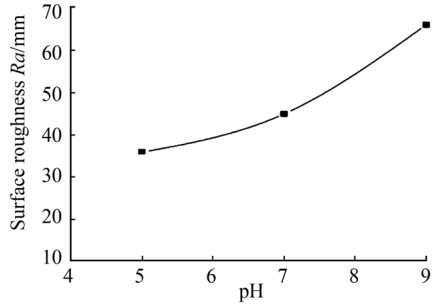

Fig. 3 Average *Ra* of ENi-P-Al_2O_3 composite deposits at different bath pH

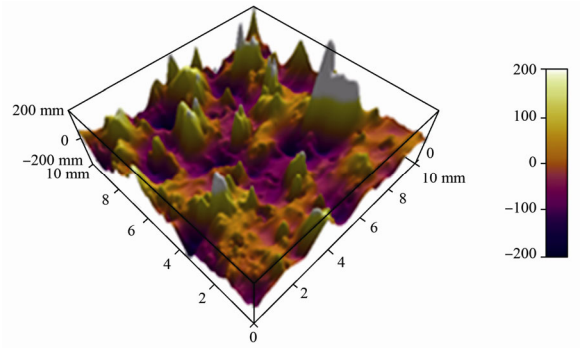

(a) Baths A

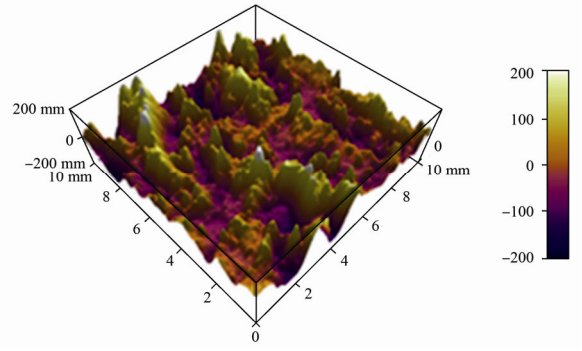

(b) Bath B

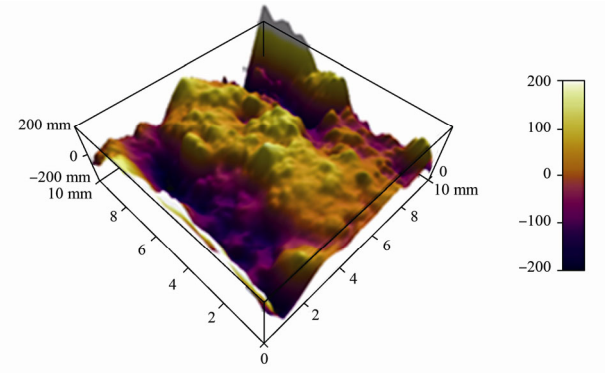

(c) Bath C

Fig. 4 AFM images of ENi-P-Al_2O_3 composite deposit

These substrates had an initial average surface roughness of 11 nm. By comparing the values, it is evident that all specimens have different surface roughness values due to the different growth pattern of the deposit. The results show that the Ra value increases with increase in bath pH value, which confirms that more amount of alumina particles are embedded or incorporated into the deposit during the deposition process as the bath pH increases from 5 to 9. Thus the affect of pH on the average surface roughness is a vital consideration for Naval Architects and Marine Engineers while designing marine components like hull surface, pipes etc.

ENi-P deposits have considerably higher microhardness values than the conventional electroplated nickel (Gawrilov, 1979; Mallory and Hajdu, 1990). It is therefore attributable to the said that ENi-P deposits have found applications in many industrial streams. The hardness levels of ENi-P-Al_2O_3 composite deposits depend largely on the percentage of alumina particles present in the deposit. Fig. 5 graphically shows the variation in microhardness of as deposited ENi-P-Al_2O_3 composite deposits at different bath pH. The microhardness values of the as-deposited substrates at different bath pH have been represented in Table 2. The result reflects that microhardness increases as the value of bath pH increases. The deposit obtained in bath C (pH 9) shows maximum microhardness value of 625 Hv in as deposited condition, as against a minimum microhardness value of 261 Hv of deposit obtained in bath A (pH 5). The higher microhardness obtained in composite deposits is due to double strengthening effect from the dispersion strengthening of hard phase and precipitation strengthening of Ni-P alloy (Balaraju and Seshadri, 1999). It may be noted that the microhardness value of non deposited MS specimen is measured to be as 220 Hv, which is considerably lower than the as-deposited specimens. Increase in hardness is thus based on the bath pH, which further controls the particle incorporation on the deposit, thereby affecting the microhardness and hence the material properties.

This aspect can go a long way in ensuring optimum design of marine components like fasteners, nuts, bolts, screws and washers, which form an integral and vital part of any marine vessel.

On analysing Fig. 6 and Table 2, it is observed that the deposition rate increases to a maximum value of 24.57 μm/h as the bath pH increases from 5 to 9. This implies that as the pH of the chemical bath increases, there is greater particle incorporation onto the substrate, and hence increasing the deposition rate or the deposition thickness.

The deposition thickness obtained for as-deposited substrates from baths A, B and C are 16.38, 27.30 and 32.76m respectively. Fig. 7 shows the FESEM of cross section of the deposition or film thickness of as-deposited substrates obtained from baths A, B and C. Greater incorporation of particles result in larger quantities or mass fraction of alumina, Ni and P into the as-deposited substrates. As already mentioned, microhardness values exhibited by ENi-P deposits are notably higher than the microhardness values of the conventional electroplated nickel, and for ENi-P-Al_2O_3 composite deposits, it is the alumina particle concentration in the ENi-P matrix that controls the hardness levels. From the results obtained, it is revealed that as the bath pH increases from 5 to 9, the alumina incorporation into the as-deposited substrates also increases. This hence results in greater microhardness values of the as-deposited substrates obtained from bath C, followed by deposits obtained from bath B and A respectively. It may be noted that the property of wear resistance of the as-deposited substrate is outlined or defined by the adhesive wear failure and high microhardness of deposits (Staia *et al.*, 1996; Gawne and Ma, 1987). Hence, it may be submitted that as-deposited substrates with greater alumina incorporation would exhibit higher microhardness values along with greater wear resistance. This may also be summed up by submitting that as the deposition rate or deposition thickness increases, the microhardness and hence the wear resistance of the as-deposited substrates also increases.

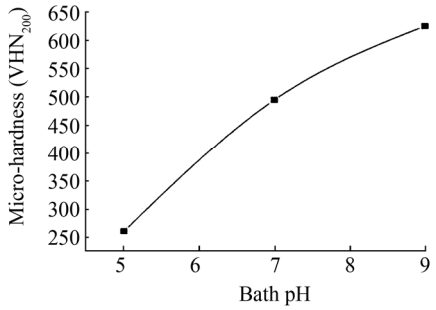

Fig. 5 Microhardness value of ENi-P-Al_2O_3 composite deposits at different bath pH

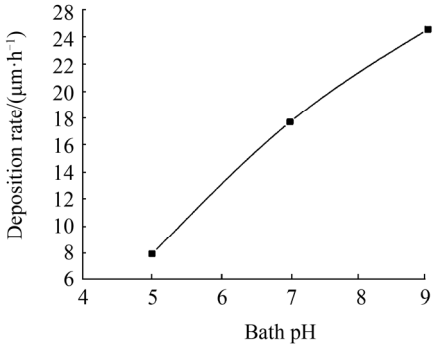

Fig. 6 Deposition rate of ENi-P-Al_2O_3 composite deposits at different bath pH

The effect of increasing bath pH on the contact angle of ENi-P-Al_2O_3 composite deposits is shown in Table 2. Fig. 8 on the other hand represents the images of the contact angle made by a liquid drop on the as-deposited substrate surface, for deposits obtained from baths A, B and C.

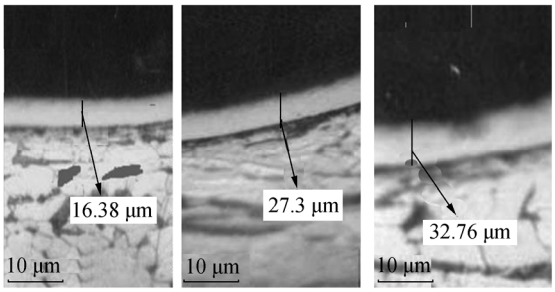

(a) Baths A (b) Bath B (c) Bath C

Fig. 7 FESEM morphology of ENi-P-Al_2O_3 composite deposit film thickness

Contact angle is the angle, conventionally measured through the liquid, where a liquid/vapor interface meets a solid surface. It quantifies the wettability of a solid surface by a liquid. Measure of the contact angle is directly proportional to the surface roughness and inversely proportional to the wettability (Mallory and Hajdu, 1990). By analyzing the contact angle values as shown in Table 2 and Fig. 8, it is revealed that deposit obtained from bath C (pH 9) has the maximum average contact angle value of 99.2° and the deposit obtained from bath A (pH 5) has the minimum contact angle of 77.2°. This also implies that the deposit with higher contact angle has a greater roughness and vice versa (Athauda *et al.*, 2012; Shirtcliffe *et al.*, 2010). Hence, the contact angle was found to increase with increasing bath pH, thereby increasing the average surface roughness (*Ra*) and decreasing the wettability of the composite deposit.

Wear resistance property is defined by adhesive wear failure and high microhardness of deposits (Sudagar *et al*., 2012; Dervos *et al.*, 2004). The deposits obtained at different bath pH were examined for wear resistance using a normal load of 20 N at a speed of 100 r/min. Resistance to wear was thereafter analyzed from the scratches formed onto the deposited surface by the movement of roller. Fig. 9 shows the FESEM images of worn surface morphology of as-deposited composite deposits obtained from bath A, B and C, respectively.

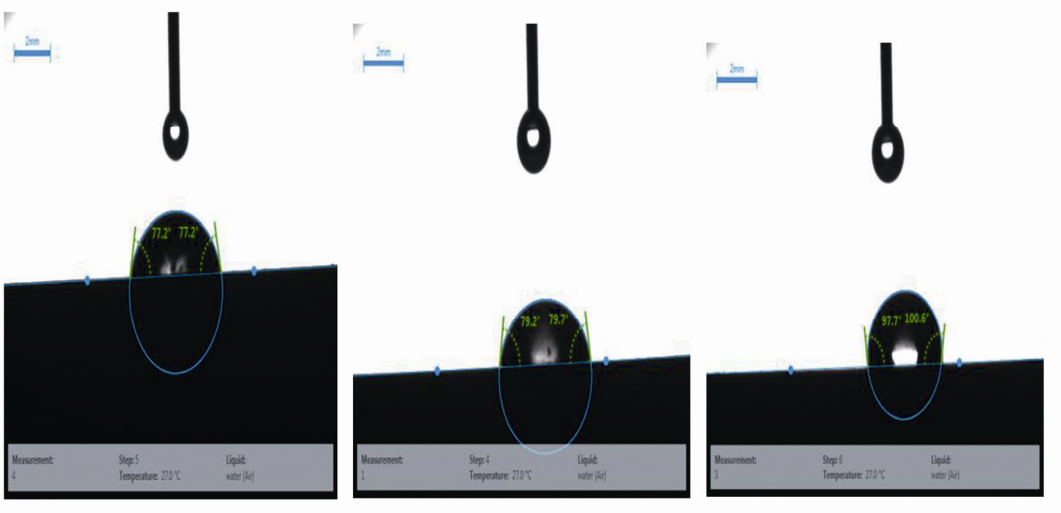

(a) Baths A (b) Bath B (c) Bath C

Fig. 8 Contact angle images of ENi-P-Al_2O_3 composite deposits

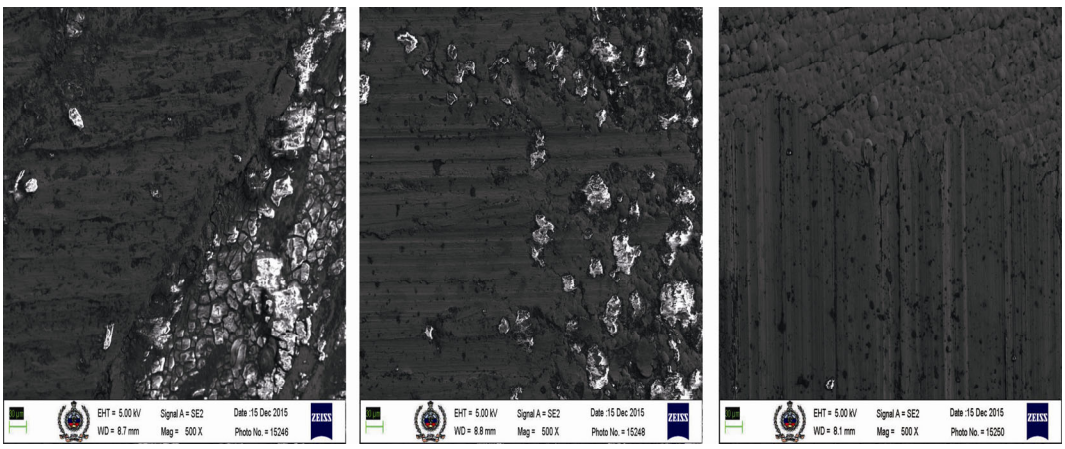

(a) Baths A (b) Bath B (c) Bath C

Fig. 9 FESEM images of worn surface morphology of as- deposited composite deposits

It is clearly indicative that the deposit obtained from bath C shows the least scoring marks as compared to deposits obtained from bath A and bath B. Maximum scoring is observed in deposit obtained from bath A. In the wear versus time plot of bath A, bath B and bath C (Fig. 10), we can see that the graph of bath C indicates better wear resistance as compared to baths A and B. This thereby reflects that the adhesive wear failure (known as prows) of the deposit obtained from bath C is minimum, hence leading to better wear resistance property.

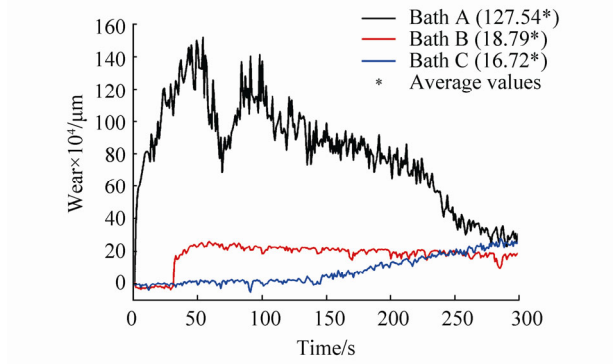

Fig. 10 Wear of as-deposited condition of composite deposits obtained from baths A, B and C

The same is also attributable to the high microhardness value possessed by the deposit obtained from bath C, thereby ensuring better wear resistance of the deposited sample. Fig. 11 shows the coefficient of friction of composite deposits obtained at different bath pH using a pin-on-disc tester.

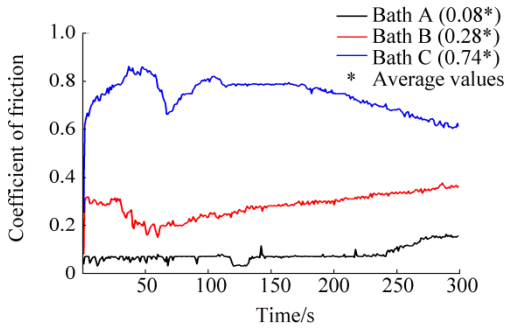

Fig. 11 Coefficient of friction of as-deposited condition of composite deposits obtained from baths A, B and C

Deposit obtained from bath C exhibits maximum coefficient of friction of 0.74 as compared to deposits obtained from baths A and B exhibiting values 0.08 and 0.28 respectively.

Fig. 12 depict the corrosion rate vs. pH of the as-deposited specimens obtained from Salt Water Spray Chamber respectively. The corrosion rate thus obtained for as-deposited ENi-P-Al_2O_3 composite deposited specimens from baths A, B and C reveals that the specimen from bath C has the least corrosion rate or maximum corrosion resistance, followed by the specimen from bath B and bath A respectively. The values of corrosion rate obtained for as-deposited ENi-P-Al_2O_3 composite deposited specimens from baths A, B and C on being subjected to salt spray for 240 hours are 67.67, 45.11 and 19.91 mm/a respectively. Corrosion rate for the non deposited MS specimen on the other hand had a value of 180 mm/a, thereby reflecting that the corrosion rates of specimens subjected to ENi-P-Al_2O_3 composite deposition were way lower than those of the non deposited MS specimens. This is clearly indicative of the fact that appropriate control of the bath pH can lead to a sharp reduction in the corrosion rate of the as-deposited specimens, as it is the pH that controls the amount of phosphorous and other particle incorporation into the deposit, thus controlling the corrosion levels (Gawrilov, 1979; Mallory and Hajdu, 1990), thereby enhancing the material or substrate property and improving service life in humid/marine environment and for underground pipeline laying applications. Increase in the corrosion resistance of the as-deposited substrate is thus attributable to the increase in the phosphorous content in the deposit (Sudagar *et al*., 2013), in addition to the incorporation of non-corrosive alumina (Alirezaei *et al*., 2004; Balaraju *et al*., 2006), both of which are eventually controlled by the bath reactivity or bath pH.

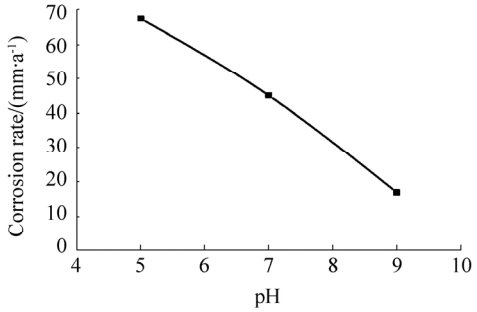

Fig. 12 Effect of pH on the corrosion rate

4 Conclusions

The bath pH plays a critical role in determining the characteristics of the deposit. Based on the present experimental investigations, the following specific conclusions are drawn:

Microhardness of deposit obtained from bath C is 184% higher than that of the non deposited MS sample. This is attributable to the fact that at higher pH, uniform deposition of fine nickel particles over substrate surface occurs. Further, lower bath pH (pH 5) also resulted in lower levels of average *Ra*. The average surface roughness of ENi-P-Al_2O_3 composite deposits has increased from 36 nm to 66 nm as the value of bath pH has been increased from 5 to 9. Maximum deposition rate has been observed at pH 9 as against pH 5 at which the deposition rate is minimum. It indicates that maximum particle incorporation occurs at pH 9. Contact angle of the composite deposit was found to increase with increasing bath pH, thereby increasing the average *Ra* and decreasing the wettability. Deposit obtained from bath C shows the least scoring marks as compared to deposits obtained from bath A and bath B. This clearly

indicates that the composite deposit obtained from bath C or pH 9 has the maximum wear resistance and coefficient of friction. A notable reduction of 90% in the corrosion rate was observed in the deposit obtained from bath C (pH 9) in comparison to non deposited MS specimen. Increase in the corrosion resistance of the as-deposited substrate is attributable to the increase in the phosphorous content in the deposit, in addition to the incorporation of non-corrosive alumina, both of which are eventually controlled by the bath reactivity or bath pH.

Hence, this aspect of reduced corrosion rate or increased corrosion resistance of MS specimen on being subjected to ENi-P-Al_2O_3 composite deposition, along with variation in bath pH, and hence increase in alumina and phosphorous content in the as-deposited substrate can be effectively utilized for applications in humid/marine environments, with better service life of components, and at lower failure rates.

References

Aal AA, Zaki ZI, Hamid ZA, 2007. Novel composite coatings containing (TiC–Al_2O_3) powder. *Materials Science and Engineering*, **447**(1-2), 87-94.
DOI: 10.1016/j.msea.2006.10.036

Alirezaei SH, Monirvaghefi SM, Salehi M, Saatchi A, 2004. Effect of alumina content on surface morphology and hardness of Ni–P–Al_2O_3 electroless composite coatings. *Surface and Coatings Technology*, **184**(2-3), 170-175.
DOI: 10.1016/j.surfcoat.2003.11.013

Apachitei I, Duszczyk J, Katgerman L, Overkamp PJB, 1998. Particles co-deposition by electroless nickel. *Scripta Materialia*, **38**(9), 1383-1389.
DOI: 10.1016/S1359-6462(98)00053-0

Athauda TJ, Decker DS, Ozer RR, 2012. Effect of surface metrology on the wettability of SiO_2 nanoparticle coating. *Materials Letters*, **67**(1), 338-341.
DOI: 10.1016/j.matlet.2011.09.100

Balaraju JN, Kalavatib, Rajam KS, 2006. Influence of particle size on the microstructure, hardness and corrosion resistance of electroless Ni–P–Al_2O_3 composite coatings. *Surface & Coatings Technology*, **200**(12-13), 3933-3941.
DOI: 10.1016/j.surfcoat.2005.03.007

Balaraju JN, Sankara TSN, Seshadri SK, 2003. Electroless Ni–P composite coatings. *Journal of Applied Electrochemistry*, **33**(9), 807-816.
DOI: 10.1023/A;1025572410205

Balaraju JN, Seshadri SK, 1999. Preparation and characterization of electroless Ni-P and Ni-P-Si composite coatings. *Transactions of the Institute of Metal Finishing*, **77**(2), 84-86.

Baudrand DW, 1994. *Electroless Nickel plating, surface engineering*. ASM Hand Book, Vol. 5. American Society for Materials, Material Park, 290.

Campestrini P, Westing EPM, Hovestad A, De Wit JHW 2002. Investigation of the chromate conversion coating on Alclad 2024 aluminium alloy: effect of the pH of the chromate bath. *Electrochimica Acta*, **47**(7), 1097-1113.
DOI: 10.1016/S0013-4686(01)00818-0

Dervos CT, Novakovic J, Vassiliou P, 2004. Electroless Ni-B and Ni-P coatings with high fretting resistance for electrical contact applications. *IEEE Holm Conference on Electrical Contacts & the International Conference on Electrical Contacts*, 281-288.

Gawne DT, Ma U, 1987. Wear mechanisms in electroless nickel coatings. *Wear*, **120**(2), 125-149.
DOI: 10.1016/0043-1648(87)90063-9

Gawrilov GG, 1979. *Chemical (electroless) Nickel plating*. Portcullis Press, Redhill, 108-125.

Ger MD, Hwang BJ, 2002. Effect of surfactants on co-deposition of PTFE particles with electroless Ni-P coating. *Materials Chemistry and Physic*s, **76**(1), 38-45.
DOI: 10.1016/S0254-0584(01)00513-2

Grosjean A, Rezrazi M, Bercot P, 2000. Some morphological characteristics of the incorporation of silicon carbide SiC particles into electroless nickel deposits. *Surface and Coatings Technology*, **130**(2-3), 252-256.
DOI: 10.1016/S0257-8972(00)00714-3

Hanna F, Hamid AZ, Aal AA, 2003. Controlling factors affecting the stability and rate of electroless copper plating. *Materials Letters*, **58**(1-2), 104-109.
DOI: 10.1016/S0167-577X(03)00424-5

Islam M, Azhar MR, Fredj N, Burleigh TD, 2013. Electrochemical impedance spectroscopy and indentation studies of pure and composite electroless Ni–P coatings. *Surface & Coatings Technology*, **236**, 262-268.
DOI: 10.1016/j.surfcoat.2013.09.057

Islam M, Azhar MR, Fredj N, Burleigh TD, Oloyeda OR, Almajid A, Shah SI, 2015a. Influence of SiO_2 nanoparticles on hardness and corrosion resistance of electroless Ni–P coatings. *Surface & Coatings Technology*, **261**, 141-148.
DOI: 10.1016/j.surfcoat.2014.11.044

Islam M, Azhar MR, Khalid Y, Khan R, Abdo HS, Dar MA, Oloyeda OR, Burleigh TD, 2015b. Electroless Ni-P/SiC nanocomposite coatings with small amounts of SiC nanoparticles for superior corrosion resistance and hardness. *Journal of Materials Engineering and Performance*, **24**(12), 4835-4843.
DOI: 10.1007/s11665-015-1801-x

Mallory GO, Hajdu B, 1990. *Electroless plating: Fundamentals and applications*. American Electroplaters and Surface Finishers Society, Orlando, 57-101.

Sahoo P, Das SK, 2011. Tribology of electroless nickel coatings-A review. *Materials and Design*, **32**(4), 1760-1775.
DOI: 10.1016/j.matdes.2010.11.013

Shirtcliffe NJ, McHale G, Atherton S, Newton MI, 2010. An introduction to superhydrophobicity. *Advances in Colloid and Interface Science*, **161**(1-2), 124-138.
DOI: 10.1016/j.cis.2009.11.001

Staia MH, Castillo EJ, Puchi ES, Lewis B, Hintermann HE, 1996. Wear performance and mechanism of electroless Ni-P coating. *Surface and Coatings Technology*, **86-87**(2), 598-602.
DOI: 10.1016/S0257-8972(96)03086-1

Sudagar J, Jiang Q, Jiang ZH, Li GY, Elansezhian R, 2012. The performance of surfactant on the surface characteristics of electroless nickel coating on magnesium alloy. *Progress in Organic Coatings*, **74**(4), 788-793.
DOI: 10.1016/j.progcoat.2011.10.022

Sudagar J, Lian J, Sha W, 2013. Electroless nickel, alloy, composite and nano coatings–A crtical review. *Journal of Alloys and Compounds*, **571**, 183-204.
DOI: 10.1016/j.jallcom.2013.03.107

Syed S, 2006. Atmospheric corrosion of materials. *Emirates Journal for Engineering Research*, **11**(1), 1-24.